International Journal of Pharmaceutics 421 (2011) 258–268

Contents lists available at SciVerse ScienceDirect

International Journal of Pharmaceutics

journal homepage: www.elsevier.com/locate/ijpharm

Supercritical fluid assisted atomization introduced by an enhanced mixer for micronization of lysozyme: Particle morphology, size and protein stability

Zhe Du, Yi-Xin Guan*, Shan-Jing Yao, Zi-Qiang Zhu

Department of Chemical and Biological Engineering, Zhejiang University, Hangzhou 310027, China

ARTICLE INFO

Article history:
Received 3 June 2011
Received in revised form 8 September 2011
Accepted 2 October 2011
Available online 6 October 2011

Keywords:
Supercritical fluid assisted atomization
Hydrodynamic cavitation mixer
Lysozyme
Micronization
Bio-activity

ABSTRACT

Supercritical fluid assisted atomization introduced by hydrodynamic cavitation mixer (SAA-HCM) was used to produce lysozyme microparticles with controlled particle size distribution in the range for aerosol drug delivery. The process is based on the atomization effect of carbon dioxide. The solubilization of certain amount of carbon dioxide in the solution plays the key role and the HCM can intensify mass transfer between carbon dioxide and liquid feedstock greatly. Water was used as the solvent to solubilize lysozyme and thus no organic residual was detected. The influences of process parameters on particle formation were investigated including temperature in the precipitator, pressure and temperature in the mixer, concentration of the solution and feed ratio CO_2/solution. The particles were characterized with respect to their morphologies and particle size: well defined, spherical and separated particles with diameters ranging between 0.2 and 5 μm could be always produced at optimum operating conditions. Bio-activity assay showed that good activity maintenance of higher than 85% for lysozyme was usually achieved. Solid state characterizations were further performed to investigate the changes of lysozyme in the process. Fourier transform infrared spectroscopy indicated that no change in secondary structure had occurred for processed lysozyme. X-ray diffraction analysis showed that the lysozyme particles produced remained similarly amorphous as the raw material. Differential scanning calorimetry and thermogravimetry analysis revealed that there was no significant difference in water association but with the increase of water content after processing.

© 2011 Elsevier B.V. All rights reserved.

1. Introduction

Micro- and submicro-particles with narrow particle size distributions centered in different diameters are widely used in many fields such as materials, catalysts, electronics, cosmetics, dyestuffs, pharmaceuticals, *etc*. Protein and peptide drugs have been one of the most rapidly growing pharmaceuticals in last two decades due to the superior effect and specificity in curing many maladies (van de Weert et al., 2005). Presently, proteins and peptides are mainly delivered parenterally, which causes great harm to veins or tissues and receives very poor patient compliance. Pulmonary delivery has been considered as a promising noninvasive method which is an alternative to the present administrations. Lungs have extremely large surface area and thin lung epithelia deep inside, which makes the absorption of proteins much easier compared with other non-invasive routes like nasal, dermal or oral (Patton and Byron, 2007; Yang et al., 2007). Normally, for the formulation for pulmonary delivery, *i.e.* aerosol delivery formulation, the efficient particle size that can be delivered into deep lungs should be between 1 and 5 μm, or more strictly, 1 and 3 μm (Reverchon, 2003; Reverchon and Della Porta, 2003). Therefore the control of particle size is essential to produce particles suitable for aerosol delivery.

Micronizing techniques based on supercritical fluids (SCFs) have been developed for many years, which include the rapid expansion of supercritical solutions (RESS) (Chang and Randolph, 1989; Matson et al., 1987), the particles generation from gas saturated solutions (PGSS) (Kerc et al., 1999; Sencar-Bozic et al., 1997) and the supercritical antisolvent precipitation (SAS) (Chang et al., 2008; Muhrer and Mazzotti, 2003; Reverchon, 1999; Yeo et al., 1993). The precondition of RESS process is that the solute must have a good solubility in SC-CO_2. However, most of the proteins with therapeutic effect are water soluble and have very limited solubility in SC-CO_2. For PGSS process, the substance has to be heated up to melt to get the particles, which goes against the thermal stability of proteins. SAS process has been successfully applied for micronization of substances dissolved in organic solvents and attempted for protein micronization (Chang et al., 2008; Muhrer and Mazzotti, 2003; Yeo et al., 1993). However, CO_2 hardly has any anti-solvent effect on aqueous solutions because the very low solubility of CO_2 in water (Takenouchi and Kennedy, 1964; Wiebe, 1941). As a rule, water is excluded from solvents to dissolve proteins and organic solvents have to be introduced, hence the residue of organic solvent becomes

* Corresponding author. Tel.: +86 571 87951982; fax: +86 571 87951982.
E-mail address: guanyx@zju.edu.cn (Y.-X. Guan).

0378-5173/$ – see front matter © 2011 Elsevier B.V. All rights reserved.
doi:10.1016/j.ijpharm.2011.10.002

a problem when operating SAS process and the bio-activity of proteins may be denatured. Moreover, the particle size control of the process is not favorable enough for aerosol drug delivery.

In recent years, utilization of solubilization of SC-CO_2 in the solution to assist atomization has brought about a novel SCF based micronizing technique, which is named supercritical fluid assisted atomization (SAA) (Reverchon, 2002). This process used a thermostated saturator to implement solubilization of CO_2 in the solution of substance and a thin wall injector to induce the atomization of the solution into a precipitator to form particles. The forming of particles is characterized by the pneumatic atomization to form primary droplets, the decompressive atomization caused by the fast release of CO_2 from primary droplets to form smaller secondary ones and the "one droplet one particle" mechanism. This novel technique can be used not only for systems of organic solvent and drugs but also for aqueous solutions of water-soluble drugs. SAA process has been successful in micronizing of antibiotics and polymers from either organic solvent or water with controlled particle size distributions (Li et al., 2009; Reverchon, 2002, 2003, 2004; Reverchon and Antonacci, 2006; Reverchon and Della Porta, 2003) and most recently this process has been studied for protein micronization (Adami et al., 2009; Rodrigues et al., 2009). Fine particles were produced, but the final addition of ethanol could be unfavorable for protein micronization.

In 2008, Cai et al. evaluated the importance of solubilization of CO_2 in solution in the processes of SCF based atomization, and introduced the hydrodynamic cavitation phenomenon that was familiar in fluid machinery and fluid transportation but offered a new approach of enhanced mixing of SCF and solution. This process was called supercritical fluid assisted atomization introduced by hydrodynamic cavitation mixer (SAA-HCM) (Cai et al., 2008). SAA-HCM process can be considered as an improvement of SAA process. In SAA-HCM process, the enhanced mixer is basically a vessel consisting of two 316 stainless steel flanges sealed with an O-Ring, where a copper orifice plate is used as the mixing point. This orifice plate serves firstly to withhold the flows for sufficient premixing of solution and SC-CO_2, and then to bring in the hydrodynamic cavitation. When the premixed fluid flows through the orifice, the pressure variation at the throat of sieve plate cause CO_2 to convert into transient gas bubbles. Thus the liquid region generates a number of CO_2 cavities, which subsequently collapse owing to the recovery of the pressure after the orifice. Cavitation happens, resulting in a convective and enhanced mixing. Cai et al. successfully produced micro- and submicro-particles of antibiotics including levofloxacin hydrochloride and roxithromycin with controlled size distributions. The effect of the enhanced mixer to form smaller particles and narrower size distributions was confirmed compared with those produced with the absence of the mixer. Wang et al. (Wang et al., 2010) and Miao et al. (Miao et al., 2010) were also successful in producing fine microparticles of sodium cellulose sulfate and Ginkgo flavonoids using the SAA-HCM process, respectively. The feasibility of using water as the sole solvent and the capability of particle size control makes SAA-HCM process very promising in protein micronization.

In this work, lysozyme was used as a model protein because its structure and properties have been well determined and it has been widely used in many studies on SCF based techniques (Adami et al., 2009; Chang et al., 2008; Muhrer and Mazzotti, 2003; Sellers et al., 2001). The aim of this work is to investigate the feasibility of SAA-HCM process in micronization of lysozyme and provide data that are useful for later studies on other proteins micronization. It is well known that protein has the bio-activity and is sensitive to temperature and pressure. The aqueous solution of protein has relatively high viscosity and is apt to bubble and thus may cause some disturbances on the micronization process. Therefore, the range of parameters selecting for good morphologies of protein particles, high activity maintenance and process stability become more troublesome. Here we study the influences of parameters on particle morphology, size and size distribution as well as the effect of process on the bio-activity and structure of lysozyme.

2. Experimental

2.1. SAA-HCM apparatus

Fig. 1 gives a schematic description of the SAA-HCM process. It is characterized by three feed lines, for supercritical CO_2, the solution and hot N_2, respectively, as well as three vessels: the mixer, the precipitator, and the condenser. CO_2 was stored in a cylinder and released into the system at gas state through a valve. The gaseous CO_2 firstly passed through a filter to remove any impurities, and then entered into the cooling bath (DFY-20L/30, Yuhua) to achieve a set temperature to ensure a liquid flow of CO_2. Liquid CO_2 was then sent to the high pressure pump (P-200A, Thar) to pressurize, and heated in a heating bath (DF-101S, Changcheng) before sent into the mixer. Liquid solution in a glass vessel was pumped

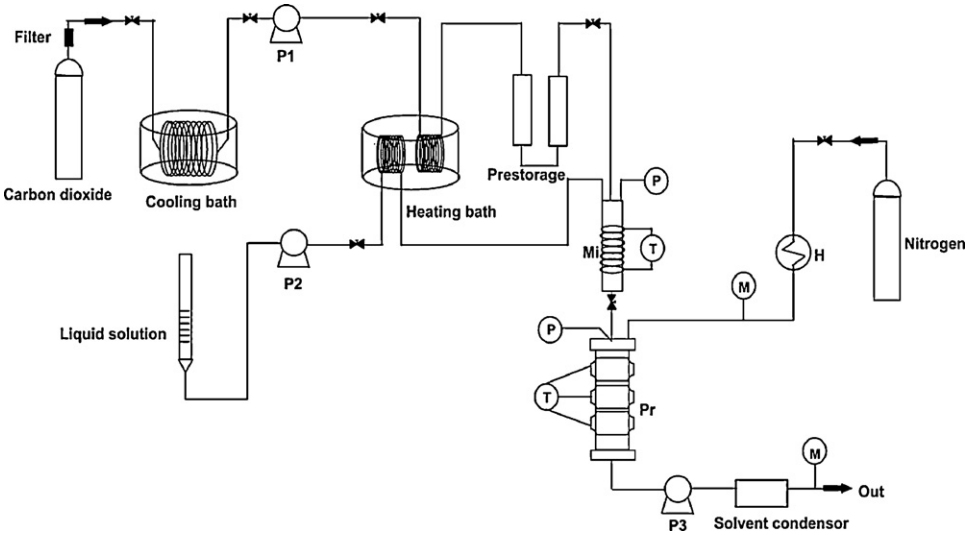

Fig. 1. Schematic diagram of the supercritical fluid assisted atomization introduced by hydrodynamic cavitation mixer (SAA-HCM) process (H, nitrogen heater; P_1 and P_2, pumps; P_3, vacuum pump; M_i, mixer; and P_r, precipitator).

by a high pressure pump (J-W, ZJSH), electrically heated and sent into the HCM where SC-CO_2 contacted with the solution. The pressure and temperature in the mixer was maintained. The mixture was then sent to a thin-wall stainless steel injector (i.d. 200 μm) located in the stainless steel precipitator to generate atomization at near atmospheric pressure. N_2 was taken from a cylinder, heated by an electric heat exchanger (NQD, ZJ-Dros) and sent into the precipitator with a flow rate of 20 L/min to assist the evaporation. The precipitator was electrically heated and the temperature was controlled. A vacuum pump was connected to the exit of the precipitator to maintain a certain pressure in it. The particles were then collected by a stainless steel filter with a 0.5 μm pore size at the bottom of the precipitator. The mixture of CO_2, N_2 and solvent vapor then passed through a cooling unit to condense the solvent. The overall flow rate of the rest (CO_2 and N_2) was measured and the exhaust was let into the atmosphere.

2.2. Materials

Lysozyme was purchased from Sangong Biological Engineering and Service Co. Ltd. (Shanghai, China). The commercial lysozyme powder was spray-dried product, which consisted of collapsed micro-particles with size ranging from 5 to 20 μm. Food grade CO_2 and N_2 with the purity above 99.0% were purchased from Jingong Gas Co. Ltd. (Hangzhou, China). Ethanol was obtained from Hangzhou Chemical Reagent Co. Ltd. (Hangzhou, China). *Micrococcus lysodeikticus* ATCC 4698 was purchased from Sigma (USA). Lysozyme has an isoelectric point of 10.7. It was directly solubilized into water to prepare lysozyme stock solution.

2.3. Analytical methods

2.3.1. Particles morphology and size

Samples of the particles produced were observed by a scanning electron microscope (SEM, JSM-6390A, JEOL) and SEM images were conducted with particle image analysis software (Nano Measurer, Department of Chemistry, Fudan University) for PSD calculation. 1000 target particles were considered in each PSD calculation performed.

2.3.2. Biological activity assay

In this assay, 20 mg of *M. lysodeikticus* was added to 20 ml of phosphate buffer (pH 6.98, 1/15 mol/L), ground and filtrated to prepare a bacterial suspension. The suspension was then heated to 25 °C prior to use. The absorption of the suspension was firstly adjusted to 0.65–0.67 using the same phosphate buffer as a reference. Lysozyme powders were solubilized into the buffer at a same concentration of 0.1 mg/ml, respectively. The biological reaction was initiated by adding 10 μl of each enzyme solution to 3 ml of the bacterial suspension, respectively. The decrease in the absorption rate (ΔA) at 450 nm in 2 min was monitored using a UV–vis spectrophotometer (Ultrospec 3300 pro, GE Healthcare). ΔA was proportional to activity of lysozyme. Three assay replicates per sample were performed.

2.3.3. Fourier transform infrared spectroscopy (FT-IR)

Lysozyme powders were mixed with anhydrous KBr and compressed into a film with an evacuable die. The films were placed directly into the nitrogen-purged sample chamber of the spectrophotometer (Tensor27, Bruker) to be analyzed. 256 scans between 400 and 4000 cm^{-1} with resolution of 4 cm^{-1} were co-added. Spectra of water vapor and carbon dioxide were subtracted from the protein spectra according to previously established standard (Dong et al., 1990, 1995). Spectra were smoothed with a seven-point Savitzky–Golay smoothing function to avoid possible noises.

2.3.4. X-ray powder diffraction (XRD)

Lysozyme samples were analyzed with a XRD apparatus (X'Pert PRO, PANalytical). The generator voltage was 40 kV and the tube current was 40 mA. Angles (2θ) varied from 3° to 70° at 2°/min. Cu was used for anode material.

2.3.5. Differential scanning calorimetry (DSC)

DSC analyses were performed using a differential scanning calorimeter (Pyris DSC 7, Perkin Elmer). Samples of commercial lysozyme and lysozyme particles (5–7 mg) were sealed in aluminium pans with vented lids and loaded in sample cells under nitrogen, and then scanned from 25 to 230 °C at 10 °C/min.

2.3.6. Thermogravimetric analysis (TGA)

TGA analyses were performed with a thermogravimetric analyzer (Pyris 1 TGA, Perkin Elmer). Samples of commercial lysozyme and lysozyme particles (3–13 mg) were loaded on an open platinum TGA pan suspended from a microbalance and heated from 25 to 275 °C at 10 °C/min under nitrogen.

3. Results and discussion

As discussed previously on SAA and SAA-HCM processes, the solubilization of CO_2 in the solution is one of the key factors to determine the efficiency of the process. In this observation, the operating point with respect to the phase equilibria of the ternary system of solvent/CO_2/solute should be well decided. In the case of protein aqueous solution, the lack of data for ternary system water/CO_2/protein has become a barrier for approaching a good dissolution condition. Since the binary system water/CO_2 has been well determined, the data of the phase equilibria of the binary

Table 1
Process parameters of experiments performed on lysozyme.

	PT (°C)	*P* (MPa)	MT (°C)	*C* (g/L)	*R* (CO_2/solution)
Effect of solvent composition					
75% ethanol	70	10	70	1	2.2
50% ethanol	70	10	70	1	2.2
25% ethanol	70	10	70	1	2.2
15% ethanol	70	10	70	1	2.2
Effect of PT					
Water	60	9.5	70	3	1.8
Water	90	9.5	70	3	1.8
Water	120	9.5	70	3	1.8
Effect of *P*					
Water	90	8.5	70	3	1.8
Water	90	9.5	70	3	1.8
Water	90	10.5	70	3	1.8
Water	90	12.5	70	3	1.8
Effect of MT					
Water	90	9.5	40	3	1.8
Water	90	9.5	50	3	1.8
Water	90	9.5	70	3	1.8
Water	90	9.5	80	3	1.8
Water	90	9.5	90	3	1.8
Water	90	9.5	120	3	1.8
Effect of *C*					
Water	90	9.5	70	1	1.8
Water	90	9.5	70	2	1.8
Water	90	9.5	70	3	1.8
Water	90	9.5	70	4	1.8
Water	90	9.5	70	5	1.8
Water	90	9.5	70	15	1.8
Effect of *R*					
Water	90	9.5	70	3	1.8
Water	90	9.5	70	3	1.5
Water	90	9.5	70	3	1.2
Water	90	9.5	70	3	0.9

PT: precipitator temperature; *P*: mixer pressure; MT: mixer temperature; *C*: solution concentration; and *R*: flow ratio CO_2/solution.

system may be applied to predict the operating points based upon the hypothesis that the presence of the protein does not strongly affect the phase behavior. As calculated referring to the data of equilibria from literature (Takenouchi and Kennedy, 1964; Wiebe, 1941; Wiebe and Gaddy, 1939), the operating points of the solution–CO_2 mixture would always drop into the two-phase region and the CO_2 rich phase contains very little water and negligible amount of solute. Hence the pressure and temperature in the mixer should serve to determine the composition of the phases formed, and the flow ratio CO_2/solution would show negligible effect on the composition of final mixture. Considering that the presence of protein in the solution may modify the phase equilibria (VLEs), and also due to the specific characteristics of protein solutions, empirical data on the influence of the above three parameters should be necessary. Besides, the precipitator temperature and the solution concentration are studied in detail in this work. Furthermore, the possibility of using ethanol as co-solvent to increase the solubility of CO_2 in solution is evaluated. All experimental conditions used are listed in Table 1.

3.1. Production of micro-particles of lysozyme

3.1.1. The presence of ethanol as the co-solvent

Due to the poor solubility of CO_2 in water, different fractions of ethanol were added in preliminary experiments to evaluate the possibility of adding ethanol as co-solvent to increase the solubility of CO_2 and the effect of ethanol on process stability and particles morphology. As shown in Fig. 2, deflated lysozyme spheres and doughnut like particles were observed. While ethanol fraction decreased, particles produced tended to be spherical in shape. Ethanol has relatively low boiling point and specific heat than water, which make the evaporation much easier. When ethanol was used as the co-solvent, the fast evaporation of solvent allowed most of the solute to precipitate on the surfaces of the droplets. That is because mass transfer rate of lysozyme from condensed surfaces to the nuclei of the droplets is slower than the effect of surface condensation. The relatively low diffusivity of biological macromolecules could even strengthen this effect. Thus the early precipitation formed hollow shells that would be apt to collapse. Furthermore, the rapid evaporation of solvent caused a small amount of CO_2 to remain in the particles after water totally evaporated. Some cavities formed when CO_2 was released after the solid particles had already formed. These two effects above caused the particles produced to collapse or even shape like doughnuts. When ethanol fraction decreased, evaporation became modest and particles tended to be spherical in shape. Since the imperfect morphology and the low retain of bio-activity (relative activity of around 60%) using ethanol as the co-solvent, water was used as the sole solvent in the following experiments. Another important reason to use pure water as the solvent is that no organic residual would be induced.

3.1.2. Effect of precipitator temperature

Normally the precipitator temperature (PT) determines the efficiency of solvent evaporation. Fig. 3 shows the SEM images of particles produced at different precipitator temperatures. It can be observed that when PT was lower, some coalescence between particles happened. The particles produced at the PT of 90 °C were well separated spheres. When PT was raised to 120 °C, some particles tended to collapse and were formed as deflated ones. The possible explanation of the coalescence is that operating at a PT

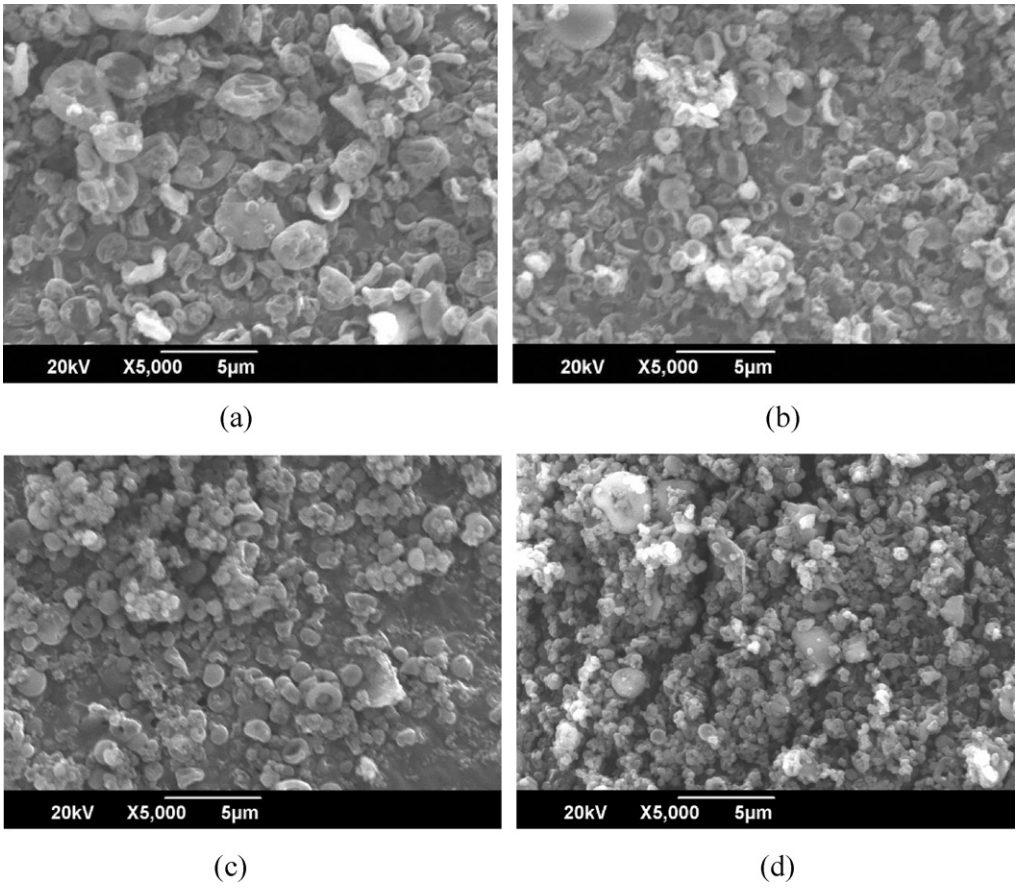

Fig. 2. Lysozyme particles micronized at precipitator temperature of 70 °C, pressure of 10 MPa and temperature of 70 °C in the mixer, concentration of 1 g/L, flow ratio CO_2/solution of 2.2. (a) 75% ethanol, (b) 50% ethanol, (c) 25% ethanol, and (d) 15% ethanol.

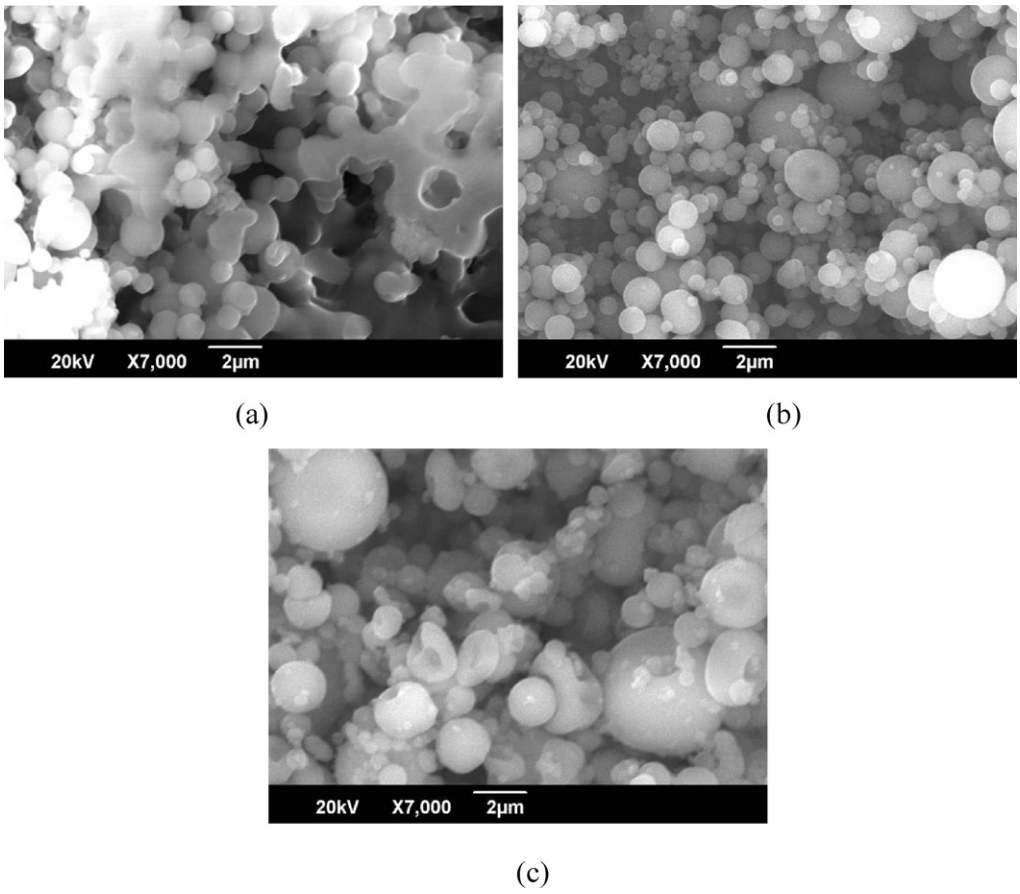

Fig. 3. Lysozyme particles produced from aqueous solution at pressure of 9.5 MPa and temperature of 70 °C in the mixer, concentration of 3 g/L, flow ratio CO_2/solution of 1.8 and precipitator temperature of (a) 60 °C, (b) 90 °C, and (c) 120 °C.

of 60 °C did not offer an efficient evaporating of water, and would lead to recondensation of water on collected particles. In fact, the powders collected when operating at the PT of 60 °C were damp, and the amount were smaller than those collected at other PTs. The reason was that the inefficient evaporating allowed the solution to be pushed through the stainless steel filter, containing part of the solute in it. When operating at the PT of 120 °C, the relatively high temperature caused very fast evaporating of water and particles produced tend to collapse. Since the effect was not strong, only a slight collapse on some particles was observed. Accordingly, to obtain efficient water evaporation and well shaped particles, also to avoid thermal effect on bio-activity, we always use 90 °C as the precipitator temperature.

3.1.3. *Influence of the temperature in the mixer*

Fig. 4 shows the SEM images of lysozyme particles produced at different mixer temperature (MT) ranging from 40 °C to 120 °C. From these images, a strong effect of mixer temperature on the morphologies of the particles can be observed. When mixer temperature varied from 40 °C to 70 °C, the morphologies remained the same and at the operating temperature range, well defined, spherical and separated particles were obtained. However, we noted that as MT increased to 80 °C, particles began to collapse and obviously deflated ones showed up, even some formless objects were observed. The shape of the particles further deteriorated as MT continued to increase. However, no significant changes in size could be observed. The temperature in the mixer is a key parameter that can influence the properties of protein since the residence of protein in the apparatus mostly happens in the mixer. The reasonable explanation of the change in morphology is due to the thermal denaturation of lysozyme. It is possible that the denaturation caused the lysozyme in solution to precipitate in the mixer before depressurization into the precipitator. The solid suspended in the solution and disturbed the atomization, causing the imperfect particles and even formless objects. The suspending precipitates were also collected at the stainless steel filter.

MT affected on particles size in two aspects. On the one hand, as MT increased, the CO_2 content in the solution decreased and the effect of dissolved CO_2 on the viscosity and the surface tension of the solution weakened. On the other hand, the increase of MT directly reduced the viscosity and the surface tension of the solution. These two aspects could be comparable and thus the intensity of the atomization did not change a lot, leading to the similar particle size.

3.1.4. *Influence of the pressure in the mixer*

Lysozyme particles were produced at different mixer pressures ranging from 8.5 to 12.5 MPa to investigate the influences on particle morphology and size. Spherical well defined particles were obtained as shown in Fig. 3(b), which is corresponding to pressure of 9.5 MPa. Mean particle diameters of the samples at different mixer pressures were 1.014, 0.920, 0.850 and 0.713 μm, respectively. In the application of drug delivery, the amount of the drugs delivered into the body is directly proportional (*via* density) to the total volume of drugs. Hence, cumulative distributions of particles size in terms of volume percentage of particles are displayed in Fig. 5. Narrowing of distributions can be observed as *P* increased. To explain the influence of pressure in the mixer, the change of CO_2 content in the solution with respect to the phase equilibria should be considered. With the increase of pressure, the fraction

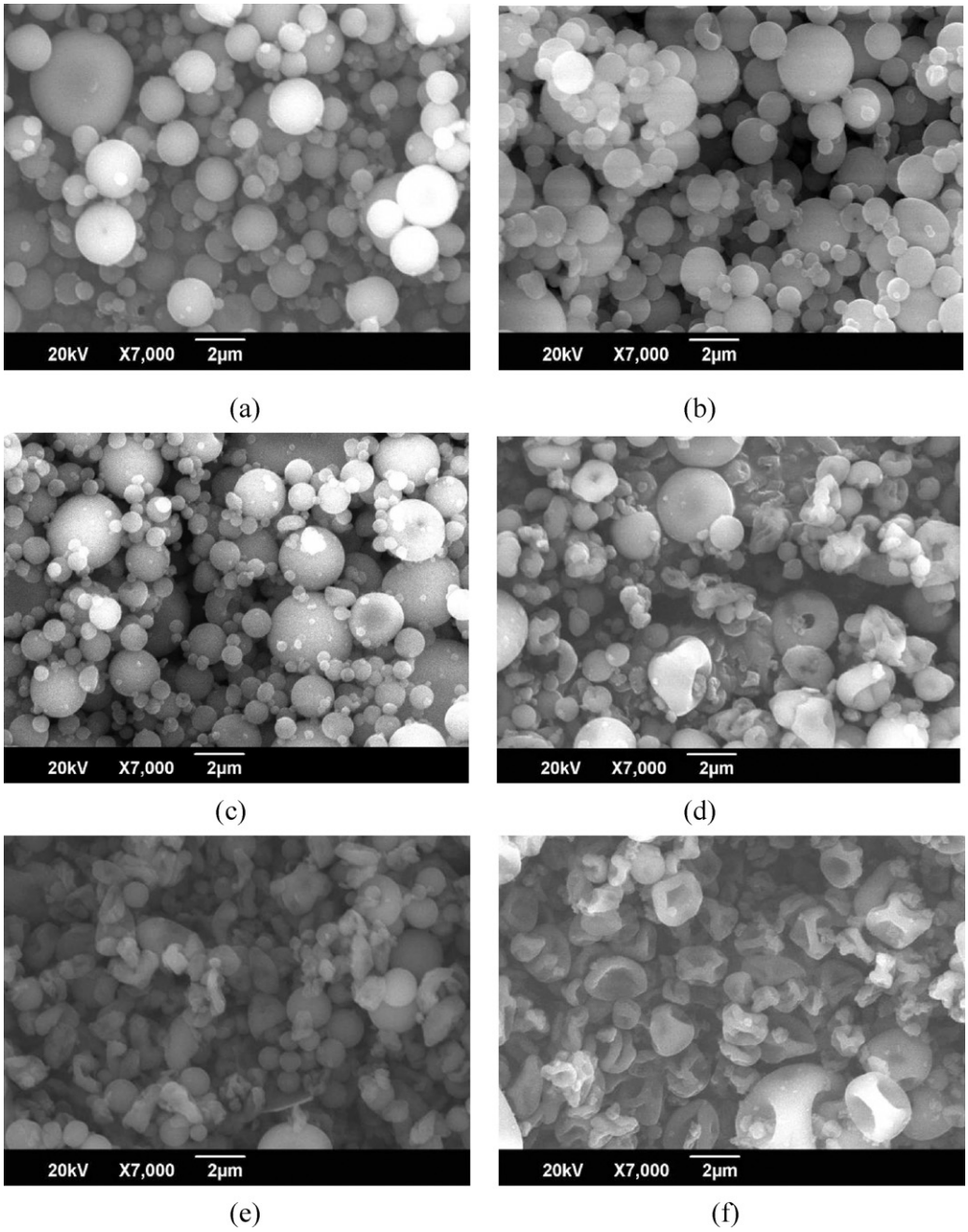

Fig. 4. Lysozyme particles produced from aqueous solution at precipitator temperature of 90 °C, mixer pressure of 9.5 MPa, concentration of 3 g/L, flow ratio CO_2/solution of 1.8, and mixer temperature of (a) 40 °C, (b) 50 °C, (c) 70 °C, (d) 80 °C, (e) 90 °C, and (f) 120 °C.

of CO_2 in solution became higher, the viscosity and the surface tension of the mixture in the mixer reduced subsequently. According to the theory of aerodynamic interaction and unstable wave growth (Reitz and Bracco, 1982; Yan et al., 2004), the reduced surface tension and viscosity induced more violent atomization which resulted in smaller primary droplets. Meanwhile, the larger content of CO_2 also enhanced the release of CO_2 from primary droplets and the formation of the secondary droplets became more drastic. Therefore, smaller secondary droplets formed and led to smaller particles according to the "one droplet-one particle" mechanism. Finally, the PS decreased and the PSD became narrower. The distribution curve for pressure of 10.5 MPa seemed to broaden compared with that for pressure of 9.5 MPa, and thus it moved rightwards. This should attribute to the complexity of atomization at higher pressure, where agglomeration resulting from the collision among droplets formed some large particles (Li et al., 2009).

From Fig. 5, we know that at 8.5 MPa, 71% of lysozyme particles lied in the range of 1–3 μm (the most restrictive limits for aerosol drug delivery), and only 9% by volume of the particles had a diameter smaller than 1 μm. And that 73%, 75% and 59% by volume of the particles produced lied in the range of 1–3 μm at 9.5 MPa, 10.5 MPa and 12.5 MPa, respectively.

3.1.5. *Influence of the solution concentration*

Fig. 6 shows the SEM images referring to lysozyme particles produced under different solution concentrations (*C*) ranging from 1 g/L to 15 g/L. An increase of particle size and polydispersity can be observed. With the increase of C, particles produced began to collapse slightly, particularly at concentration beyond 5 g/L. According

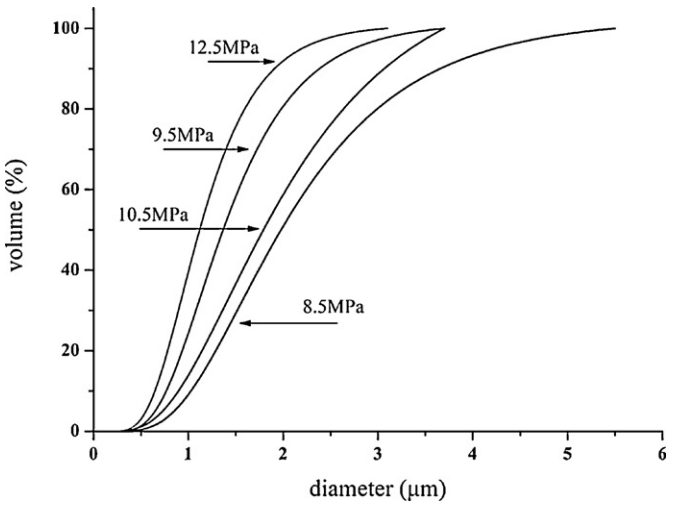

Fig. 5. Cumulative distribution curves of lysozyme particles produced at different mixer pressure in terms of volume percentage.

to the analysis, the mean particles size ranged between 0.771 and 1.760 μm as *C* increased from 1 g/L to 15 g/L. Fig. 7 gives the distributions of particles size in terms of volume percentage of particles, a broaden of distributions can be observed as C increases. This change in particle size and particle size distribution is a typical phenomenon observed in many SAA and SAA-HCM processes (Cai et al., 2008; Reverchon, 2003; Reverchon and Antonacci, 2006). The solution concentration affected the viscosity and the surface tension of the solution. These two parameters increased when higher concentrations were employed, and the atomization thus was weakened. Therefore, larger droplets were produced and larger particles were precipitated and the distributions broadened. As the diameters of the droplets increased, the drag coefficient between the droplets and the gas phase increased, causing imperfect droplets surfaces and thus deflated particles. Also, as larger particles were produced, they were much easier to be affected by the flow of gas and were apt to collapse. According to the distribution curves in Fig. 7, at concentration of 1 g/L, up to 35% by volume of the particles produced have diameters smaller than 1 μm. With the increase of *C*, the percentage by volume of particles with diameter of 1–3 μm rises to 73% and 78% at concentration of 3 g/L and 4 g/L, respectively. When protein concentration was increased to 15 g/L, only 39% by volume of the particles are in the range 1–3 μm, and even 24% of them are larger than 5 μm.

3.1.6. Influence of the flow ratio CO_2/solution

Lysozyme particles produced at different flow ratio CO_2/solution (*R*) ranging from 1.8 to 0.9 were well defined and separated spherical particles as shown in Fig. 3(b), which is corresponding to *R* of 1.8. The effect of *R* on the particle size is not as distinct as that using organic solvents (Reverchon, 2004). As discussed before, the operating points of this process always dropped into the two phase region of the phase equilibia diagram when using water as solvent and the effect of *R* on phase composition could be neglected.

3.2. Influences of process parameters on enzyme activity

Due to the operating temperature and high pressure employed in this work, maintenance of protein activity is another issue to be considered. To determine the effects of process parameters on activity, assays employing the characteristic reaction catalyzed by lysozyme were performed. Enzyme activity was expressed as relative activity (RA) to unprocessed lysozyme as the reference.

3.2.1. Effect of the pressure in the mixer

Fig. 8 gives the relative enzyme activity of lysozyme samples produced at *P* ranging from 8.5 to 12.5 MPa. There is an obvious loss of RA at high pressure of 12.5 MPa. According to Toews et al. (Toews et al., 1995), when exposed to CO_2 at 20 MPa and 70 °C, the pH of aqueous solution decreased to 2.95. The reduced pH can cause irreversible changes in structure of proteins, including the quantities of α-helix, when exposed to compressed CO_2. Also, exposure of protein solution in high pressure can cause the protein to be more vulnerable to temperature. Nevertheless, it is abnormal that the samples produced at a pressure of 8.5 MPa, slightly higher than the critical point, exhibited an obvious low RA. This needs further experiments to understand.

3.2.2. Effect of the temperature in the mixer

Fig. 9 gives the relative enzyme activity of lysozyme samples produced at MT ranging from 40 to 120 °C. No consistent trend of RA has been observed as MT varied. As discussed before, the deformation of particles in the cases of higher MT may be due to the denaturation of lysozyme in the mixer. However the result of bio-activity assay shows that at MTs 80 and 90 °C, no significant denaturation (RA > 90%) occurred. A possible explanation is that at our experimental MTs, the precipitation due to the denaturation was reversible because of the relatively short residence time. Some more experiments were employed, showing that lysozyme can sustain a period of time when heating up to 100 °C without significant loss in bio-activity (RA > 95%). When MT increased to 120 °C, lysozyme could not maintain activity any more and a great loss occurred (RA < 35%).

3.2.3. High activity maintenance of lysozyme

The parameter PT is also essential to the maintenance of bio-activity of protein because the thermal stress on the protein during precipitation may cause denaturation of protein. Our results show that PTs under 100 °C almost had no impact on the bio-activity. But higher PT for example 120 °C strongly decreased the relative activity of lysozyme to 53%. The solution concentration and flow ratio CO_2/solution did not present obvious effects on the activity of lysozyme (data not shown). In all cases of our experimental conditions, RAs of above 85% had been obtained. Therefore, except for the conditions of extreme temperatures and pressures, SAA-HCM could provide good bio-activity maintenance of lysozyme. This owes to the relatively mild temperatures that can be employed and the absence of organic solvent and therefore, the broad feasibility of selection of parameters could be achieved.

3.3. Characterization of lysozyme micro-particles

3.3.1. Fourier transform infrared spectroscopy

FT-IR has been widely used to study the secondary structure of proteins. The secondary structure of unprocessed and SAA-HCM processed lysozyme was examined by the comparison of FT-IR spectra at amide I (1600–1700 cm^{-1}) and amide III (1200–1350 cm^{-1}) regions that are characteristic of proteins. Fig. 10 shows the spectra of unprocessed and SAA-HCM processed lysozyme at a condition of PT of 90 °C, *P* of 9.5 MPa, MT of 70 °C, *C* of 3 g/L and *R* of 1.8. The strong peak around 1656 cm^{-1} for unprocessed commercial lysozyme and processed lysozyme particles has been observed due to the high content of α-helix (Fu et al., 1994; Sellers et al., 2001). For processed lysozyme, no new peaks and relevant peak shifts can be observed in the amide I and III regions, indicating no modification from commercial protein. Inverted secondary derivative curves (not shown) indicated little increase in β-sheets content and some decrease in α-helix content compared in amide I region. Accordingly, SAA-HCM process does not destroy the secondary structure and maintained the

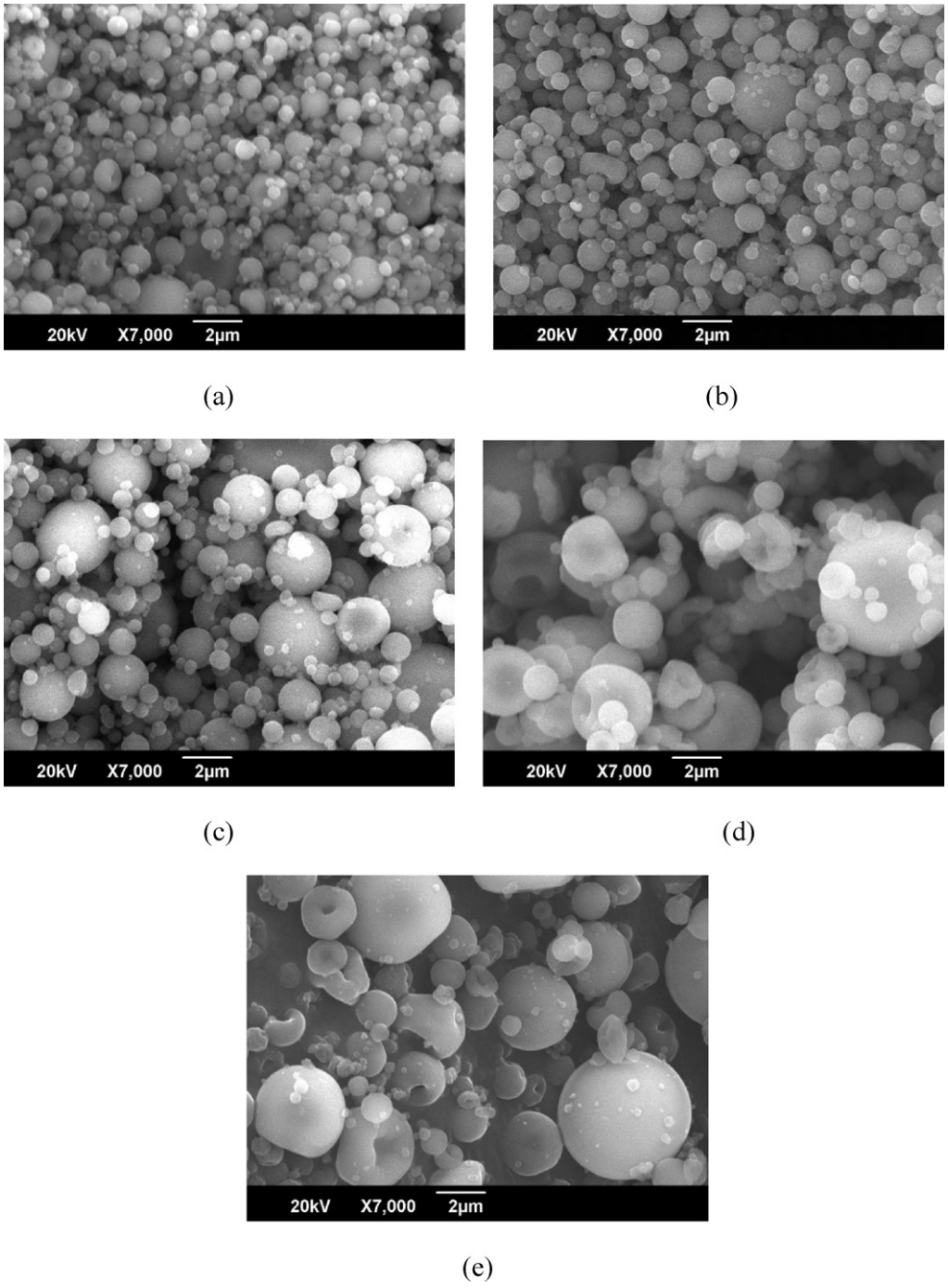

Fig. 6. Lysozyme particles produced from aqueous solution at precipitator temperature of 90 °C, pressure of 9.5 MPa and temperature of 70 °C in the mixer, flow ratio CO_2/solution of 1.8, and concentration of (a) 1 g/L, (b) 2 g/L, (c) 3 g/L, (d) 5 g/L, and (e) 15 g/L.

conformational integrity of lysozyme fairly well. This result is identical with the good maintenance of bio-activity.

3.3.2. X-ray powder diffraction

XRD analyses of unprocessed and processed lysozyme particles were performed to evaluate the occurrence of eventual structural changes at the crystal level. As shown in Fig. 11, low crystallinity was observed for both the samples. As described before, the unprocessed commercial lysozyme was obtained using spay-drying. Thus, SAA-HCM gives the same amorphous particles as the spray-drying. This result is also consistent with other SAA processes (Reverchon and Antonacci, 2006; Reverchon and Della Porta, 2003). The phenomenon of formation of amorphous protein particles in SAA-HCM process is attributed to the dominant intramolecular attraction during solution supersaturation.

3.3.3. Differential scanning calorimetry

DSC analysis was performed to determine the thermal activity of lysozyme and the data obtained could offer an evaluation of the changes in thermal properties and water association. The DSC curves of lysozyme exhibit two endotherms as shown in Fig. 12. One is broadly positioned at 45–150 °C, the other with different width is at about 200 °C. The endotherm at higher temperature was considered to indicate the denaturation transition with some

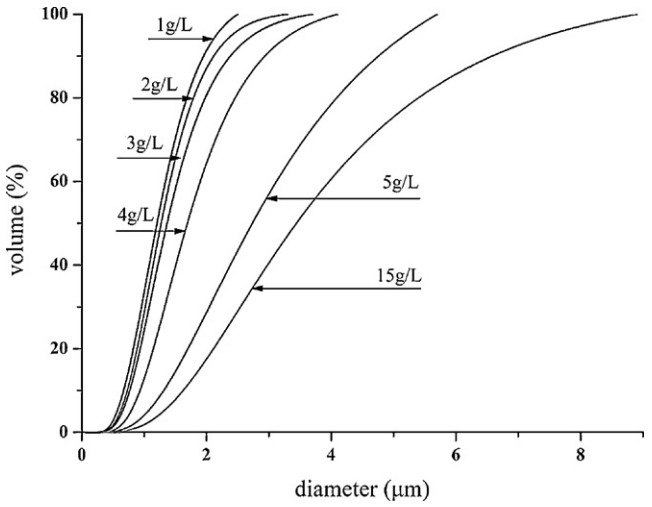

Fig. 7. Cumulative distribution curves of lysozyme particles produced at different concentrations in terms of volume percentage.

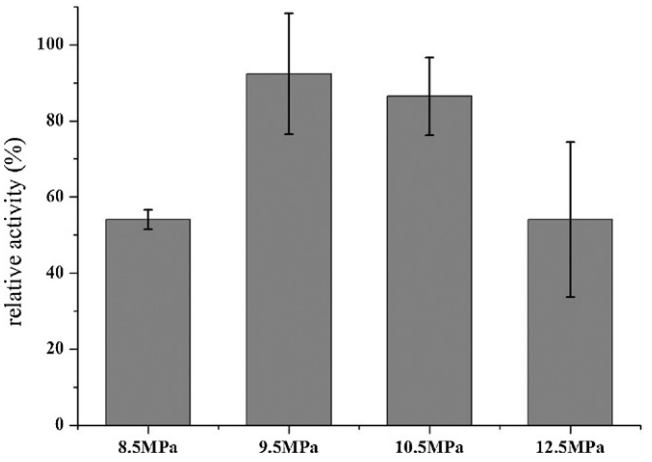

Fig. 8. Relative activity of lysozyme produced from aqueous solution at different mixer pressure.

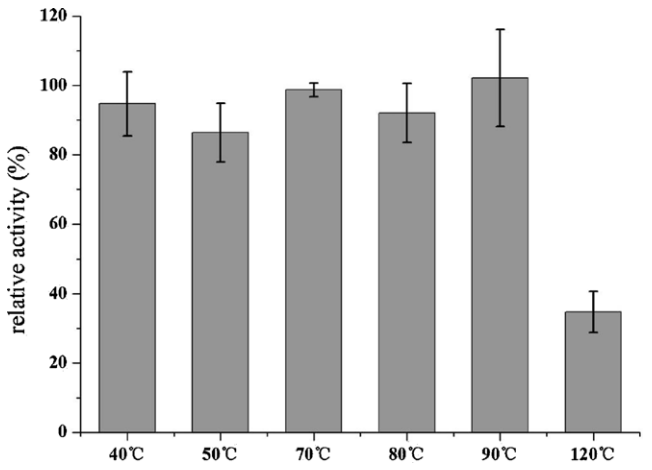

Fig. 9. Relative activity of lysozyme produced from aqueous solution at different mixer temperature.

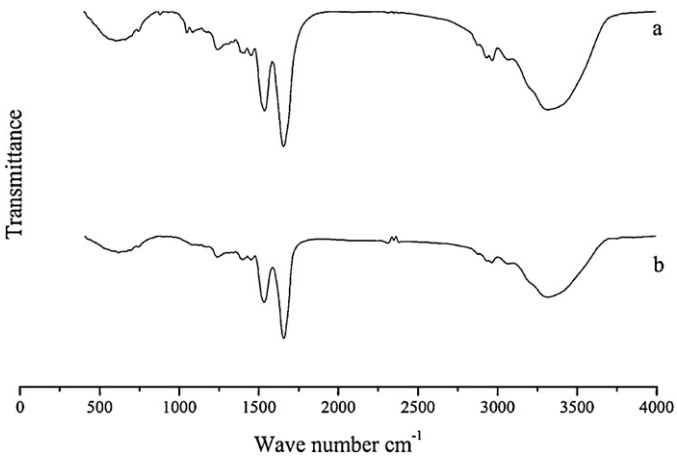

Fig. 10. FT-IR spectra of (a) unprocessed and (b) SAA-HCM processed lysozyme.

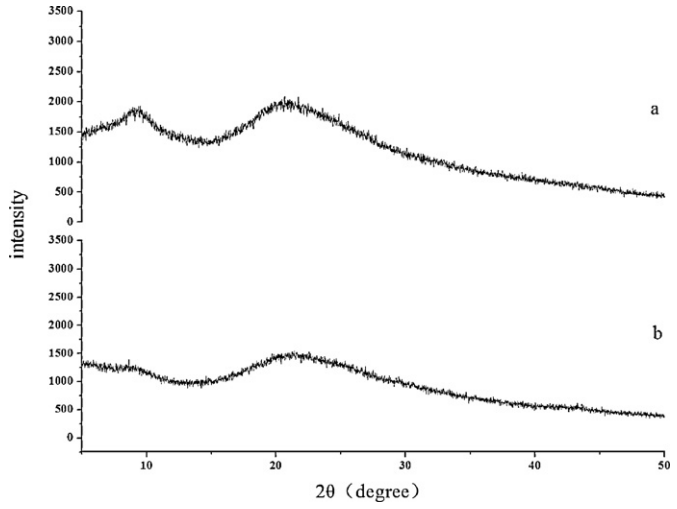

Fig. 11. X-ray powder diffraction patterns for (a) unprocessed and (b) SAA-HCM processed lysozyme.

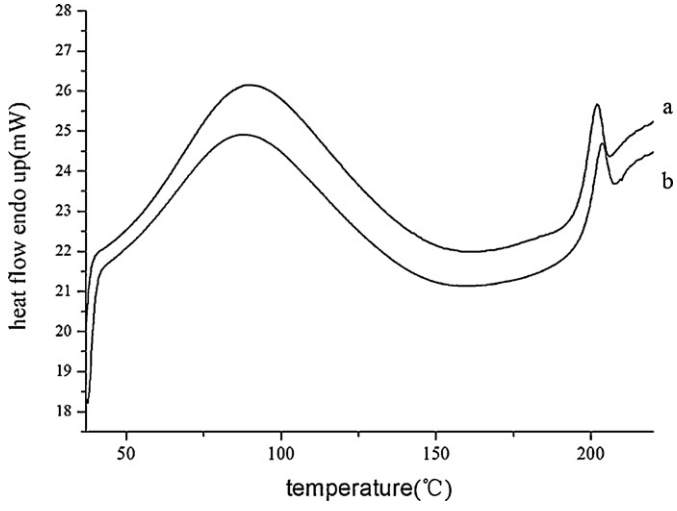

Fig. 12. DSC thermograms of (a) unprocessed and (b) SAA-HCM processed lysozyme.

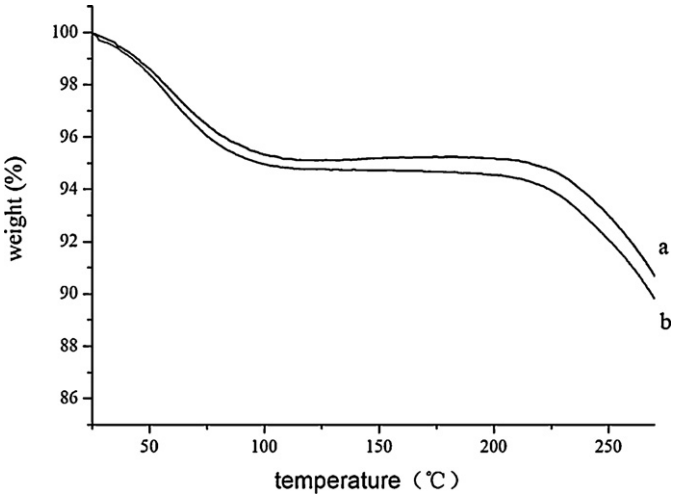

Fig. 13. TGA thermal diagrams of (a) unprocessed and (b) SAA-HCM processed lysozyme.

decomposition and the extremum of the peak was considered to reflect the melting temperature (Tm). The broad endotherm reflects the heat flow with respect to the water loss. It is obvious that the SAA-HCM process did not affect the strength of association of lysozyme with water, since the water loss endotherm remained the same in the onset and end temperature.

3.4. Thermogravimetric analysis

TGA was used together with DSC for determination of weight change in thermal events as decomposition reactions. It is also helpful in determining the moisture content of samples. Fig. 13 gives the TGA curves of weight *versus* temperature. The progress of weight loss by programmed heating can be designated into three stages. The first stage starts at the beginning of heating, and is attributed to the loss of adsorbed water. The second stage is much slower than the first and is due to the following water loss. The designating of these two stages can be confirmed by DSC curves, where broad endotherms were apparently over the same temperature range as the TGA weight loss. In the third stage, weight loss begins to accelerate. This stage is due to the decomposition of the protein and thus occurred just at a temperature higher than Tm. The weight loss of the first two stages for unprocessed and SAA-HCM processed (PT of 90 °C, *P* of 9.5 MPa, MT of 70 °C, *C* of 3 g/L and *R* of 1.8) lysozyme are 4.90 and 5.54%, respectively. The higher water content can be attributed to the relatively milder temperature and shorter residence time of SAA-HCM process compared with spray-drying. Besides the milder temperature used to protect proteins from thermal denaturation, the higher water content is also favorable to maintain the bio-activity of lysozyme, as illustrated by Nagendra et al. (1998). Moreover, the loss of water begins at the same temperature for the two samples and the rates of water loss are nearly the same according to the derivative curves of TGA thermograms. This result again confirms that SAA-HCM did not change the strength of association of lysozyme with water.

4. Conclusions

Using water as the solvent, lysozyme microparticles with narrow size distributions centered at the range of particles size suitable for aerosol drug delivery are successfully produced. While offering flexible tailoring of particles size and particle size distributions of lysozyme microparticles, SAA-HCM exhibits satisfying advantages in maintaining the bio-activity of lysozyme. Further characterizations showed that this process has little impact on the secondary structure of lysozyme and the thermal behavior also remains similarly. The positive results obtained by producing lysozyme microparticles bring the possibility of SAA-HCM to produce other proteins. More experiments on different therapeutic proteins are necessary to extend the potential of SAA-HCM process.

Acknowledgement

The authors should thank gratefully for financial support provided by the National Natural Science Foundation of China (20676118, 21076185).

References

Adami, R., Osséo, L.S., Reverchon, E., 2009. Micronization of lysozyme by supercritical assisted atomization. Biotechnol. Bioeng. 104, 1162–1170.
Cai, M.Q., Guan, Y.X., Yao, S.J., Zhu, Z.Q., 2008. Supercritical fluid assisted atomization introduced by hydrodynamic cavitation mixer (SAA-HCM) for micronization of levofloxacin hydrochloride. J. Supercrit. Fluids 43, 524–534.
Chang, C.J., Randolph, A.D., 1989. Precipitation of microsize organic particles from supercritical fluids. AIChE J. 35, 1876–1882.
Chang, S.C., Lee, M.J., Lin, H.M., 2008. Role of phase behavior in micronization of lysozyme via a supercritical anti-solvent process. Chem. Eng. J. 139, 416–425.
Dong, A., Huang, P., Caughey, W.S., 1990. Protein secondary structures in water from second-derivative amide I infrared spectra. Biochemistry (Mosc) 29, 3303–3308.
Dong, A.C., Prestrelski, S.J., Allison, S.D., Carpenter, J.F., 1995. Infrared spectroscopic studies of lyophilization-induced and temperature-induced protein aggregation. J. Pharm. Sci. 84, 415–424.
Fu, F.N., Deoliveira, D.B., Trumble, W.R., Sarkar, H.K., Singh, B.R., 1994. Secondary structure estimation of proteins using the amide-III region of Fourier transform infrared spectroscopy: application to analyze calcium-binding-induced structural changes in calsequestrin. Appl. Spectrosc. 48, 1432–1441.
Kerc, J., Srcic, S., Knez, Z., Sencar-Bozic, P., 1999. Micronization of drugs using supercritical carbon dioxide. Int. J. Pharm. 182, 33–39.
Li, Z.Y., Jiang, J.Z., Liu, X.W., Tang, H.H., Wei, W., 2009. Experimental investigation on the micronization of aqueous cefadroxil by supercritical fluid technology. J. Supercrit. Fluids 48, 247–252.
Matson, D.W., Fulton, J.L., Petersen, R.C., Smith, R.D., 1987. Rapid expansion of supercritical fluid solutions: solute formation of powders, thin films, and fibers. Ind. Eng. Chem. Res. 26, 2298–2306.
Miao, S.F., Yu, J.P., Du, Z., Guan, Y.X., Yao, S.J., Zhu, Z.Q., 2010. Supercritical fluid extraction and micronization of ginkgo flavonoids from ginkgo biloba leaves. Ind. Eng. Chem. Res. 49, 5461–5466.
Muhrer, G., Mazzotti, M., 2003. Precipitation of lysozyme nanoparticles from dimethyl sulfoxide using carbon dioxide as antisolvent. Biotechnol. Prog. 19, 549–556.
Nagendra, H.G., Sukumar, N., Vijayan, M., 1998. Role of water in plasticity, stability, and action of proteins: the crystal structures of lysozyme at very low levels of hydration. Proteins 32, 229–240.
Patton, J.S., Byron, P.R., 2007. Inhaling medicines: delivering drugs to the body through the lungs. Nat. Rev. Drug Discov. 6, 67–74.
Reitz, R.D., Bracco, F.V., 1982. Mechanism of atomization of a liquid jet. Phys. Fluids 25, 1730–1742.
Reverchon, E., 1999. Supercritical antisolvent precipitation of micro- and nanoparticles. J. Supercrit. Fluids 15, 1–21.
Reverchon, E., 2002. Supercritical-assisted atomization to produce micro- and/or nanoparticles of controlled size and distribution. Ind. Eng. Chem. Res. 41, 2405–2411.
Reverchon, E., 2003. Terbutaline microparticles suitable for aerosol delivery produced by supercritical assisted atomization. Int. J. Pharm. 258, 1–9.
Reverchon, E., 2004. Erythromycin micro-particles produced by supercritical fluid atomization. Powder Technol. 141, 100–108.
Reverchon, E., Antonacci, A., 2006. Chitosan microparticles production by supercritical fluid processing. Ind. Eng. Chem. Res. 45, 5722–5728.
Reverchon, E., Della Porta, G., 2003. Micronization of antibiotics by supercritical assisted atomization. J. Supercrit. Fluids 26, 243–252.
Rodrigues, M.A., Li, J., Padrela, L., Almeida, A., Matos, H.A., de Azevedo, E.G., 2009. Anti-solvent effect in the production of lysozyme nanoparticles by supercritical fluid-assisted atomization processes. J. Supercrit. Fluids 48, 253–260.
Sellers, S.P., Clark, G.S., Sievers, R.E., Carpenter, J.F., 2001. Dry powders of stable protein formulations from aqueous solutions prepared using supercritical CO_2-assisted aerosolization. J. Pharm. Sci. 90, 785–797.
Sencar-Bozic, P., Srcic, S., Knez, Z., Kerc, J., 1997. Improvement of nifedipine dissolution characteristics using supercritical CO_2. Int. J. Pharm. 148, 123–130.
Takenouchi, S., Kennedy, G.C., 1964. Binary system H_2O–CO_2 at high temperatures and pressures. Am. J. Sci. 262, 1055–1074.

Toews, K.L., Shroll, R.M., Wai, C.M., Smart, N.G., 1995. pH-defining equilibrium between water and supercritical CO_2—influence on SFE of organics and metal-chelates. Anal. Chem. 67, 4040–4043.

van de Weert, M., Jorgensen, L., Horn Moeller, E., Frokjaer, S., 2005. Factors of importance for a successful delivery system for proteins. Expert Opin. Drug Deliv. 2, 1029–1037.

Wang, Q., Guan, Y.X., Yao, S.J., Zhu, Z.Q., 2010. Microparticle formation of sodium cellulose sulfate using supercritical fluid assisted atomization introduced by hydrodynamic cavitation mixer. Chem. Eng. J. 159, 220–229.

Wiebe, R., 1941. The binary system carbon dioxide–water under pressure. Chem. Rev. 29, 475–481.

Wiebe, R., Gaddy, V.L., 1939. The solubility in water of carbon dioxide at 50, 75 and 100 degrees, at pressures to 700 atmospheres. J. Am. Chem. Soc. 61, 315–318.

Yan, C.J., Xie, M.Z., Yin, P.H., 2004. Mechanisms of breakup and atomization of a viscous liquid jet in a viscous gas. Acta Aerodyn. Sin. 22, 422–426.

Yang, M., Velaga, S., Yamamoto, H., Takeuchi, H., Kawashima, Y., Hovgaard, L., Vandeweert, M., Frokjaer, S., 2007. Characterisation of salmon calcitonin in spray-dried powder for inhalation: effect of chitosan. Int. J. Pharm. 331, 176–181.

Yeo, S.D., Lim, G.B., Debenedetti, P.G., Bernstein, H., 1993. Formation of microparticulate protein powders using a supercritical fluid antisolvent. Biotechnol. Bioeng. 41, 341–346.